Automated Parking Surveys from a LIDAR Equipped Vehicle

Douglas A. Thornton[a,b], Dr. Keith Redmill[b], and Dr. Benjamin Coifman[b,c,d]

[a] Battelle Memorial Institute
505 King Avenue
Columbus OH, 43201
USA

[b] Electrical and Computer Engineering
The Ohio State University
2015 Neil Ave
Columbus, OH 43210
USA

[c] Civil, Environmental and Geodetic Engineering
The Ohio State University
2070 Neil Ave
Columbus, OH 43210
USA

thorntond@battelle.org
redmill@ece.osu.edu
coifman.1@osu.edu

[d] corresponding author

Abstract

Parking surveys provide quantitative data describing the spatial and temporal utilization of parking spaces within an area of interest. These surveys are important tools for parking supply management and infrastructure planning. Parking studies have typically been performed by tabulating observations by hand, limiting temporal resolution due to high labor cost. This paper investigates the possibility of automating the data gathering and information extraction in a proof of concept study using a two-dimensional scanning Light Detection and Ranging (LIDAR) sensor mounted on a vehicle, though the work is compatible with other ranging sensors, e.g., stereo vision. This study examines parallel parking in the opposing direction of travel. The ranging measurements are processed to estimate the location of the curb and the presence of objects in the road. Occlusion and location reasoning are then applied to determine which of the objects are vehicles, and whether a given vehicle is parked or is in the traffic-stream. The occupancy of the parking area, vehicle size, and vehicle-to-vehicle gaps are then measured. The algorithm was applied to an area with unmarked, on-street parking near a large university campus. Vehicle counts from 29 trips over four years were compared against concurrent ground truth with favorable results. The approach can also be applied to monitor parking in the direction of travel, eliminating the possibility of occlusions and simplifying the processing.

Keywords

Parking survey, probe vehicle, vehicle detection and measurement, curb detection

1 Introduction

A review of 11 international cities estimated that cruising for open parking spaces accounts for 30% of the total vehicular volume, causing significant congestion in central business districts and elsewhere (Shoup, 2006). Parking surfaces account for up to 40% of a typical city's land area, dramatically affecting efficient land usage (Childs, 1999). Parking consumes a considerable amount of resources while contributing to the environmental costs of passenger vehicle use. Meanwhile the topic of parking "has received comparatively little study upon which to ground our development of policies for the future," and, "[w]e do not understand nearly enough about how individuals respond to parking policy interventions nor how these responses interact with local circumstances" (Marsden, 2006). De Cerreño (2004) found that "many cities lack basic information about their parking resources." A primary contributor underlying the scarcity of knowledge about parking, and on-street parking in particular, is the effort required to obtain the requisite data through traditional, labor-intensive parking surveys.

Parking surveys, such as those applied in Deakin et al. (2004), Guo et al. (2013), and Marshall et al. (2008), are used for obtaining quantitative data to describe the usage of parking surfaces over temporal and spatial regions of interest. These surveys provide valuable information, revealing the parking needs, habits, and trends of motorists. Using this knowledge, planners can adjust current parking policies and shape future parking infrastructure to better match demand or encourage alternative transportation modes. Researchers can develop better models to set more effective guidelines (a need demonstrated by Marsden, 2006), forecast future demands, and predict individual responses to policy changes. Over-utilized areas can be addressed to properly price parking and reduce occupancy as proposed by Vickrey (1954) and analyzed in practice in by Pierce and Shoup (2013). These methods increase public satisfaction and reduce the environmental costs of drivers searching for parking spots. Further, if the data are collected and disseminated in real time, travelers looking for parking could utilize the information (e.g., Mathur et al., 2010).

On-street parking does not lend itself to easy assessment due to the vast spatial and temporal regions of interest. The conventional methodology for performing a parking survey of on-street parking is to either walk or drive through the area of interest, manually tallying the number of parked vehicles. This method is labor intensive, and typically only provides coarse measures, such as percent occupancy in a given area. Data collection costs increase greatly with the temporal resolution required. According to the Institute of Transportation Engineers (2011), estimating peak parking accumulation for some land uses, "may require spot counts at specified intervals such as every one-quarter, one-half, one, or two-hour intervals throughout the day or portions of the day in order to assure accurate data." Furthermore, "[t]he parking survey should also be sensitive to the fact that land uses may exhibit different parking trends from day to day." Conventional parking studies are poorly suited to these needs due to the significant labor requirement.

Finer detailed information can be provided by more sophisticated survey techniques such as recording license plate numbers to track turnover and parked duration per vehicle (Gray, Bell, and Kuhn, 2008; Federal Highway Administration, 2007). Several cities are starting to deploy sensors to monitor individual metered parking spots (e.g., as discussed in Pierce and Shoup, 2013). Another method employs stationary cameras observing the parking area (Alessandrelli et al., 2012; Chen et al., 2010;). Such detail comes at increased cost, limiting these studies to high-impact areas.

This paper investigates using a Light Detection and Ranging (LIDAR) sensor mounted on a vehicle in a proof of concept study to automate the conventional parking survey data collection for parallel parking areas along arterial streets. LIDAR uses laser-based ranging to measure the distance from the sensor to nearby objects, providing a precise *point cloud* of the surrounding environment at high frequency. LIDAR is seeing rapid adoption within the transportation field in areas such as the creation of accurate digital maps and the automation of bridge and pavement inspection (Olsen, 2013). The proposed algorithm

uses the point cloud to find and spatially locate vehicles parked on-street. Once the vehicles are found, we also measure their height and length. While unmarked on-street parking is studied herein, the methodology could be extended to marked on-street parking or off-street parking such as parking garages, similar to the method presented in (Wanayuth et al., 2012).

This automated vehicle presence detection promises to greatly reduce the labor of parking surveys by eliminating the human in the loop to count vehicles while simultaneously providing measures that were formerly cost prohibitive, and potentially do so in real time. By using vehicle height and length measures, turnover can be tracked anonymously, providing for the estimation of the majority of parking characteristics as defined by Lautso (1981), e.g., momentary accumulation, average accumulation, and intensity of arrivals and departures; greatly aiding in the development of parking models. With measures such as these available the various costs of the parking search problem can be reduced, e.g., as in Kokolaki et al. (2011). Techniques for programmatically determining open parking spots can be employed (e.g., Coric and Gruteser, 2013), allowing practitioners to inventory the available parking resources.

For our system the host vehicle carrying the LIDAR sensor could be a transit bus or another municipal vehicle performing ordinary duties on defined or undefined routes, further reducing the data collection costs by eliminating the need for a dedicated driver or vehicle. The cost of a sensing system could be well below $10,000 per unit, whereas instrumenting a limited access facility using traditional fixed sensors costs approximately $60,000 (Rodier and Shaheen, 2010), while the cost to conduct a conventional on-street parking survey is dictated by the man-hours necessary to observe and reduce the data.

This research develops an algorithm using real world data from an area with unmarked, on-street parking near a large university campus. This study uses an instrumented probe vehicle to examine parallel parking in the opposing direction of travel. The LIDAR returns were processed to estimate the location of the curb, find the presence of objects in the road (i.e., on the near side of the curb) and to discern which of these objects are parked vehicles. The occupancy of the parking area, individual vehicle sizes, and vehicle-to-vehicle gaps are then measured. Note that the basic approach developed herein should be compatible with many other parking configurations, e.g., surface lots, and many other ranging sensors, e.g., stereo vision (Ohashi et al., 1997), radar (Schmid et al., 2011), or emerging Around View Monitor (AVM) systems, (Suhr and Jung, 2013).

The remainder of the paper is organized as follows. First, the background of the proof of concept study is given, followed by a description of the location of the study. Next, a three-stage process for taking the raw data and converting it to meaningful measures of parking is introduced. Then, results from 29 tours through the study corridor are presented. Finally, the paper closes with conclusions and a discussion of future work.

2 Proof of Concept Study

2.1 Overview

This work develops an automated process to measure on-street parking utilization using a host vehicle's position via GPS, and ranging sensors to monitor the nearby vehicles. While ultimately it is envisioned that the ranging sensors could be mounted on a host vehicle that is already traversing the network, e.g., a transit bus or another municipal vehicle, this pilot study uses a dedicated probe vehicle equipped with multiple sensors for positioning and ranging to ambient vehicles. Four sensors are used in this research, namely: a vertically scanning LIDAR sensor on the driver's side, a differential global positioning system receiver (DGPS), speedometer measurements via the on-board diagnostics port

(OBD), and a yaw gyroscope. The latter two sensors are used for inertial navigation corrections to the DGPS measurements. The driver's side LIDAR uses a laser beam to measure the distance to surrounding objects. It scans continuously from top to bottom in a vertical plane orthogonal to the probe's heading, with a frequency of 37 Hz, an angular coverage of 180°, and a 0.5° angular resolution. The LIDAR sensor range extends to 81 m, with a radial measurement resolution of 0.01 m[1]. For validation purposes the work also uses a video camera to image the area covered by the LIDAR.

Using the driver's side LIDAR, this work monitors parking in the opposing direction. The result is a three-dimensional point cloud that can be rendered in false color based upon distance, e.g., Figure 1. Vehicles, buildings, and trees are readily apparent to the eye in this view, though subsequent steps are needed to automatically segment the vehicles. This processing must also account for occlusions from passing vehicles on the road. The occlusions from vehicles traveling in the opposite direction are typically short in duration because of high relative speed between the occluding vehicle and the probe. For multi-lane facilities, vehicles traveling in the same direction can lead to long duration occlusions if the relative speed is low. In either case, if a non-occluded view is critical, a LIDAR sensor on the passenger side could be used to provide a non-occluded view of the parked vehicles whenever the probe is in the lane adjacent to the parking lane. For same-direction monitoring like this, the present work would still apply, but the occlusion reasoning could be omitted.

2.2 Study location

The method was developed along a road with on-street parking near the Ohio State University campus in Columbus, Ohio. Specifically, northbound probe vehicle trips on Neil Avenue were used to analyze parallel parking in the southbound direction. The study area spans 1.1 km from the northern edge of the university campus at Lane Avenue, north to Dodridge Street as shown in Figure 2. Nine cross streets bisect the study area, which are used to split Neil Avenue into 10 segments. For simplicity these segments are numbered in sequential order with segment 1 being southernmost and closest to the university. Parking in the study area is unmarked, governed only by signs prohibiting parking near intersections and bus stops, and the traffic code for maintaining driveway access.

To estimate the utilization of the unmarked parking zones, first an estimate of parking capacity must be made. Using the minimum parking space from the Manual of Uniform Traffic Control Devices (MUTCD) (Federal Highway Administration, 2009), a standard parking space was defined as having a length of 6.7 m for inner spaces, and 6.1 m for edge spaces. The amount of available parking was determined by finding parking constraints such as alleyways, driveways, and parking signs, and then recording the corresponding locations. This capacity determination only needs to be done once per link, and for this study the parking the process was executed manually; however, automated methods could be employed, e.g., Coric and Gruteser (2013). Parking zones in each segment were defined as being bounded by the "no parking" signs protecting the intersection at either end. Formalizing these locations, S_s and S_e, respectively, are defined as the start and end of the segment's parking zone. A given road segment could have any number of additional constraints where parking is prohibited (e.g., driveways or time of day restrictions). The extremes of the constraints were recorded in a manner similar to the parking signs. For each of these n constraints in a given segment, the locations are defined by D_s and D_e, respectively, as the start and end of the constraint. Equation 1 was used to calculate the number of usable parking spaces.

[1] Although the sensor provides this precision, the accuracy diminishes at higher ranging or in challenging ambient lighting.

$$Spaces = f\{S_e - S_s\}, \quad \text{If no constraints in segment}$$
$$Spaces = f\{D_{s_1} - S_s\} + f\{S_e - D_{e_n}\} + \sum_{k=1}^{n-1} f\{D_{e_k} - D_{s_{k+1}}\}, \quad \text{otherwise} \tag{1}$$

where,

$$f\{x\} = \begin{cases} 0, & \text{if } x < 6.1 \\ 1, & \text{if } 6.1 \le x < 2(6.1) \\ 2, & \text{if } 2(6.1) \le x < 2(6.1)+6.7 \\ 2+\left\lfloor \frac{x-2(6.1)}{6.7} \right\rfloor, & \text{otherwise} \end{cases}$$

2.3 Methodology

There are three stages to the parking survey algorithm. Stage One estimates the position of the probe vehicle for each LIDAR scan, processes the LIDAR data, determines whether an object is detected within the scan and finds the far side curb whenever it is visible. Stage Two integrates the information from successive LIDAR scans to segment vehicles from the background and from one another. After accounting for occlusions, the algorithm reports the globally referenced location for each vehicle, as well as measuring the vehicle's length, height and heading. Stage Three takes the vehicle information and assigns them to road segments and lanes, reporting the occupancy of each parking zone, along with other measures such as vehicle-to-vehicle gap. The details of each of the three stages are presented in Sections 2.3.1 to 2.3.3. A flowchart of the methodology incorporating the three stages is shown in Figure 3.

2.3.1 Algorithm Stage One- object detection

Stage One of the algorithm is broken into several steps; the first step is to filter out any noise in the DGPS data using an extended Kalman smoother. State estimates were made from the gyroscope and speedometer using a bicycle model of the probe vehicle in two dimensions, and then corrected using the DGPS data. After smoothing, the 4 Hz positioning data were interpolated to the higher frequency LIDAR data time stamps using the Piecewise Cubic Hermite Interpolating Polynomial algorithm (Bickley 1968), which maintains smoothness along the path.

The second step of Stage One is to create a linear reference system along the route, whereby the distance, D, traveled from the start of the segment was measured. In this case the Neil-Lane intersection was defined as the origin. Using a linear reference system simplifies the task of vehicle placement and map building by reducing the analysis space to a single dimension.

The next step is curb detection, i.e., finding the edge of the road. This step is critical to accurately finding the parked vehicles since all objects of interest must be closer to the probe vehicle than the curb. Curb detection is an active body of research and relevant methodologies have been proposed for forward facing planar LIDAR sensors, angled slightly below the horizon, scanning the downstream road (e.g., Wijesoma et al., 2004; Jabbour and Bonnifait, 2008; Peterson et al., 2008; Liu et al., 2013) as well as a vertical LIDAR similar to the one employed herein (e.g., Jabbour and Bonnifait, 2006). Wijesoma et al. (2004) employ straight line segmentation and an extended Kalman filter to estimate and evolve the road boundaries. Jabbour and Bonnifait (2008) detect road boundaries by finding the peaks in the derivative of the measured height. Peterson et al. (2008) use a wavelet transform to perform detection over a variety of curb types. Liu et al. (2013) create an elevation map from which the curbs are

identified. The method proposed herein differs from the previous methods by combining the simplicity of Jabbour and Bonnifait's algorithm, with the temporal filtering of Wijesoma et al.'s algorithm to lower computational complexity. Our method differs from Jabbour and Bonnifait in that we maintain an estimate of the curb location when the curb is occluded, and our method does not rely on a significant height change at the curb.

The curb location is assumed to be unknown a priori and the algorithm takes the following steps to locate it. The algorithm processes each vertical scan of the LIDAR data individually, using a two-dimensional Cartesian coordinate system (Ψ, Ω) in the plane of LIDAR scan, where $\Psi = r \bullet \cos\theta$; $\Omega = r \bullet \sin\theta + l_h$; r and θ are range and angle, respectively, of a LIDAR return; and l_h is the height of the LIDAR sensor above ground. In this coordinate system Ψ represents the horizontal distance out from the probe and Ω represents the vertical distance relative to the fixed height from the LIDAR. To find the ground surface in the i-th scan, the j-th point is considered part of the ground surface whenever the height, Ω_{ij}, was below a maximum road height value given by Equation 2, and the distance, Ψ_{ij}, is within a curb search range given by Equation 3. Where: Rh_{max} sets the maximum allowed lateral elevation of the roadway with respect to l_h for a given location, C_{i-1} is the curb estimate from the previous scan,[2] CD_{max} sets the maximum allowed change in curb distance per iteration, CS_{min} sets the lower limit of the curb search range and CS_{max} is the upper limit to prevent the unbounded growing of the curb estimate when no curb is present (e.g., at intersections). In general, CS_{min} is chosen based upon the number of opposing travel lanes and CS_{max} should be chosen slightly to be larger than the expected maximum distance to the curb so that the filter is given sufficient time to converge to the proper curb location after curb interruptions. For the study area with one parking lane and one travel lane, CS_{min} = 4 m and CS_{max} = 10 m was used, allowing for lane widths of 4 m and a margin of 2 m for probe location within the lane; analyzing a three lane road would simply result in a CS_{max} of 14 m, or in general, a digital map containing the number of lanes on a roadway would allow for the appropriate value for CS_{max} to be chosen programmatically. The results are fairly insensitive to the remaining parameters, though the parameters used in this proof of concept were: Rh_{max} = 0.2 m and CD_{max} = 0.5 m.

$$\Omega_{ij} < Rh_{max} \tag{2}$$

$$CS_{min} < \Psi_{ij} < \max(CS_{max}, C_{i-1} + CD_{max}) \tag{3}$$

The collection of points selected by Equations 2-3 in the i-th scan is taken to be the *ground estimate* and should comprise the road surface, the curb, and a small portion of the easement (or in the presence of an occlusion, just the road surface). The points are de-trended by fitting a line to the ground estimate by a least squares slope estimate. The slope is then removed from the points in the ground estimate. This step provides tilt compensation, making the algorithm robust to the roll of the probe vehicle, and the curvature of the road surface while also eliminating the need for the LIDAR mounting angle to be calibrated separately. Figure 4a shows the raw LIDAR returns from a single scan without a parked vehicle and Figure 4b shows a different scan with a parked vehicle.

The next step is object and occlusion detection in the i-th scan. The algorithm marks the i-th LIDAR scan as having an object in the road if two or more returns with feasible vehicle height given by Equation 4 are found in the area between the curb and the probe vehicle given by Equation 5.[3] Where, to reduce false positives from non-vehicle objects and to accommodate the road slope the minimum vehicle

[2] The initial value of C_i is not critical, e.g., whenever the probe vehicle traverses an intersection the curb location is lost and the estimate goes to the maximum value, only to be rapidly reacquired within a few meters of travel on the far side of the intersection.

[3] Note that these equations use the values from the i-1 scan because C_i is only determined after this step establishes whether or not there is an occlusion in the i-th scan.

height threshold, VH_{min}, assumes that a vehicle exceeds this threshold height above the road height at the curb, Hc_{i-1}. Similarly, the maximum vehicle height, VH_{max}, is used to filter out low hanging trees and other objects suspended over the road that do not enter the region defined by Equation 4. This proof of concept study used VH_{min} = 0.5 m and VH_{max} = 2 m. The vehicle search space minimum, VS_{min}, is set to 0.5 m away from the probe. The vehicle search space maximum, VS_{max}, is set to fall 0.5 m inside the curb and is used to accommodate noise in the estimate while recognizing the fact that vehicles are typically wider than half a meter. This threshold has the added benefit that it reduces the likelihood of detecting trashcans and pedestrians close to the curb.

$$Hc_{i-1} + VH_{min} < \Omega_{ij} < VH_{max} + Hc_{i-1} \tag{4}$$

$$VS_{min} < \Psi_{ij} < C_{i-1} - VS_{max} \tag{5}$$

The process is then repeated with the parking lane excluded, using Equations 4 and 6. If two or more returns are found in this area the i-th scan is marked as having an occlusion. Where the parking lane width threshold, *PW*, was set to 3 m from the curb because a parking stall is typically 2.5 m wide, and like VS_{max}, allowing for some tolerance in our curb estimate

$$VS_{min} < \Psi_{ij} < C_{i-1} - PW \tag{6}$$

The object detection and occlusion results for each LIDAR scan are stored along with their location, D, in the linear reference system. Then, for the final step, the curb estimate, C_i, is updated for the i-th scan. If Equation 6 finds an object between C_{i-1} and the probe vehicle, then it is assumed that the curb is occluded and C_i is set equal to C_{i-1} (e.g., as illustrated in Figure 4b). Otherwise, C_i is set equal to the Ψ_{ij} corresponding to the minimum Ω_{ij} value, as denoted with a star in Figure 4a. The operation assumes that the road is designed to drain to the shoulders, which is the case in our study area. These local estimates are then filtered across samples using an infinite impulse response filter. An assumption is made that the curbs are smooth, which was the case in the study area. Upon locating the curb, the algorithm measures the road height at the curb, Hc_i, by taking Ω at C_i. As with C_i, Hc_i is filtered across samples using an infinite impulse response filter.

2.3.2 Algorithm Stage Two- integrating information across scans

While the previous stage focused on positioning and individual LIDAR scans, Stage Two assimilates the information from successive scans to extract vehicles. First, all successive scans are reviewed to find all changes in *occlusion status* and *object detection status*. A new contiguous-object is begun if the object status changes from false to true in successive scans and neither scan had an occlusion (thus, the object must be in the parking lane). If there is not already an active contiguous-object, the algorithm will also begin a new contiguous-object if the occlusion indicator changes from true to false in successive scans and the latter scan indicates an object is present (thus, the object in the parking lane must have started while that lane was occluded). In either case, an active contiguous-object will persist until the first successive scan that does not have an object or an occlusion, at which point the contiguous-object will be closed because it is clear that the parking lane is now vacant. Figure 5a shows an illustrative example for the case of a single, un-occluded vehicle. The figure shows a top-down schematic of the roadway as the probe progresses from left to right in the lane that would be immediately below the occluding lane of travel shown in the schematic. Figure 5b shows the two indicator variables versus D, the linear reference system along the roadway.

A contiguous-object may be occluded at the beginning, middle or end. Whenever the middle of a contiguous-object is occluded it is possible that the gap between two successive parked vehicles can go

unobserved, so the occluded portion is included in the contiguous-object's length. If the beginning or end of a contiguous-object is occluded, then the length of the occlusion(s) as measured by the linear reference system is excluded from the contiguous-object's length, with the stipulation that the final length cannot be less than a minimum occluded vehicle length threshold, VLO_{min}, to ensure that if the contiguous-object is a parked vehicle it will be counted in the subsequent steps.[4] This proof of concept uses VLO_{min} = 4 m. Figure 5c-d shows an example where the contiguous-object for a parked vehicle is truncated due to occlusion, as shown by the two indicator variables, while Figure 5e-f shows an example where the gap between two parked vehicles is not observed due to an occlusion. The extended and multi-vehicle contiguous-objects will be addressed shortly.

Note that it is also possible for a parked vehicle to be totally occluded, e.g., if a slow moving bus was present. We do not attempt to address total occlusions in this proof of concept study. However, due to the high mounting location of the LIDAR sensors, it was rare that occluding vehicles could have completely blocked the view of a parked vehicle.

Even in the absence of occlusions, the issue of potentially blurring vehicles together remains since occasionally two vehicles are parked so close together that the space between them falls completely between two LIDAR scans. Thus, the gap is not detected, resulting in multiple vehicles appearing as one contiguous-object even without an occlusion.

At this point a given contiguous-object may include one or more parked vehicles, or it may contain a non-vehicle object. To resolve these issues, the next step is length estimation and reasoning. The initial estimate of length is simply the distance the probe travels with the contiguous-object in the scan, or if partially occluded, the result after the occlusion reasoning above. Any contiguous-object shorter than the assumed minimum feasible vehicle length, VL_{min}, is removed, e.g., due to a trashcan or traffic cone in the parking lane. This proof of concept uses VL_{min} = 2.5 m. By removing unreasonably short targets, the methodology was made more robust at the cost of potentially eliminating motorcycles, which were infrequent in the study area. If the study area has a significant population of smaller vehicles, e.g., commuter cars, this parameter can be adjusted lower. Contiguous-object lengths greater than the assumed maximum feasible vehicle length, VL_{max}, are separated into multiple vehicles by finding the smallest integer number of vehicles that could fit in the contiguous-object length, subject to an average vehicle length less than VL_{max}. Assuming that only passenger vehicles were parked along the street, this proof of concept uses VL_{max} = 6 m. So any contiguous-object between VL_{min} and VL_{max} is considered to be a single vehicle. Under the values chosen a 7 m contiguous object would be split into two 3.5 m vehicles, and a 20 m long contiguous object would be broken into four vehicles, each 5 m long since any contiguous object longer than $3 \bullet VL_{max}$ has to contain more than three vehicles. This approach is reasonable for counting vehicles, however, if the given application demands that the bumper-to-bumper spacing or average vehicle length needs to be highly accurate, the reasoning would have to be modified to exclude the occluded objects.

After finding the contiguous-objects and splitting those longer than VL_{max}, the vehicle locations are recorded, along with their individual length, maximum height, and heading. Figure 6 shows an example of the estimated vehicle-to-vehicle gap, vehicle length, and vehicle height from one tour, each as a function of D.

2.3.3 Algorithm Stage Three- segmenting vehicles and measuring parking utilization

In this stage, the road segments obtained in Section 2.2 are combined with the vehicle locations from Section 2.3.2 to estimate vehicles per segment. For each vehicle location in the linear reference

[4] The purpose of excluding the length is to preserve an accurate count of parked vehicles over other metrics. If the length were extended, a long, slow moving occluder passing at an inopportune moment could cause the methodology to generate a phantom parked vehicle by extending a single parked vehicle's length such that the subsequent steps break the contiguous object into two vehicles.

system, the closest road segment was found. To allow for variance in the probe vehicle's localization and vehicles parking slightly outside of the parking zones, a localization tolerance, *LT*, was used, i.e., if a vehicle was in the curbside lane and was within *LT* of a parking zone it was counted towards that segment. Vehicles outside of the parking zones beyond *LT* were excluded from the count. Considering the 1 m standard deviation of the differential GPS, an *LT* of 2 m was used. With the analyzed system, out of the 1,931 parking lane vehicles found in the evaluation (presented in the next section) there were 58 occurrences where the vehicle fell outside of the parking zones. Upon review, it turns out that all of these 58 observations were identified correctly as non-parked vehicles, resulting from at two locations where the curb lane is used for through traffic at signalized intersections. The next section tabulates the number of vehicles assigned to parking zones in each segment.

Two options are available to eliminate the dependency on the differential GPS and replace it with a lower cost solution. The first is to increase the *LT* tolerance, possibly leading to more miscounts where parking lanes are shared with travel lanes. The second is to perform map matching with the LIDAR data using fixed objects along the road (e.g., buildings) as landmarks to continually correct a noisy GPS measurement, e.g., Qin et al. (2012) and Jabbour and Bonnifait (2006). This latter option has the added benefit of being very robust in urban canyons and other feature rich locations where GPS performs the worst.

3 Results

The probe vehicle regularly traversed the study area from 2008 to 2011. While the particular days are irregular, all of the tours are on weekdays, with most occurring Tuesday through Thursday. The tours are run such that the probe will pass the segment at roughly the same time of day, either in the morning or early afternoon, providing a rich data set to test the algorithm. From this data set, 29 tours were chosen at random for the parking survey. These tours come from a span of four years and encompass the entire range of times and seasons available.

The algorithm performance was compared to manually generated ground truth data recorded from observations of concurrent video data and the LIDAR point cloud. The video generated from the camera looking out of the driver's side window was used to identify the location of parked vehicles coarsely while the LIDAR point cloud outlined in Stage One was used to accurately locate vehicles relative to immobile objects (trees, signs, etc.). Table 1 shows the total number of errors per-segment, i.e., the sum of the absolute difference between the manual count and automated count over the given segment from each of the 29 tours. From this table it is apparent that the algorithm has greater error in segments 3 and 10. A potential cause for segment 3 errors is a change in road geometry where the road both widens and curves. These changes locally reduce the effectiveness of the object reasoning. This problem can be addressed by better modeling the probe vehicle's motion and orientation through space. Meanwhile, near the termination of segment 10, there is a signalized intersection with a dedicated left turn lane. The standard route is for the probe to turn right at this intersection, resulting in occlusion by vehicles traveling in the same direction, stored in the left turn lane while waiting for the left turn signal. This occlusion has been confirmed to cause errors in several cases. Comparing the LIDAR based algorithm against the ground truth across all 29 tours there was a total of 15 miscounts, yielding an error rate of 15 in 1,873 vehicles, or 0.8 percent. Figure 7 shows the distribution of errors on each segment across the 29 tours.

The frequency of occluding vehicles may impact the accuracy of the system. If the opposing flow is high, the number of occlusions may overwhelm the occlusion reasoning presented above. At the end of Section 4 we discuss several future advances that should improve performance in the presence of

occlusions.[5] The number of opposing vehicles observed and the travel time for the 29 tours was used to determine an upper bound, qm, on the true flow rate in the opposing direction, q, using Equation 7. Where n is the count of observed vehicles, t_r is the probe vehicle's travel time, and t_O is the travel time in the opposing direction. Of course accurately estimating t_O is very difficult, which is why in this work we only find the upper bound on q.[6] The maximum number of vehicles observed for a single trip was 25, with a resulting *qm* less than 600 vehicles per hour, while the average number of vehicles observed was 12 with an average *qm* than 430 vehicles per hour.

$$qm = \frac{n}{t_r} \geq \frac{n}{t_r + t_O} = q \tag{7}$$

Table 2 shows summary statistics and utilization measures across the 29 data sets, where the utilization is simply the count divided by the capacity. From these data it can be seen that close to the university campus the realized capacity provided by unmarked parking was greater than that predicted by the MUTCD parking space guidelines.[7] This result, as one would expect, reflects that demand for parking increases the closer one gets to campus, with extremely high utilization immediately adjacent to campus. To examine time of day effects an additional 21 tours, for a total of 50 tours, were used to increase sample size within each time group. These data were grouped by: morning, noon, and early afternoon. The corresponding average count and utilization for these time groups are shown in Table 3. A dip in demand is observed during the noon hour in segments 6 through 8.

As noted previously, the LIDAR based methodology can provide details not typically collected in parking surveys, including the vehicle-to-vehicle gap, vehicle length (subject to the assumptions above) and height of the parked vehicles as shown for a single tour in Figure 6 and by histograms over the 29 tours in Figure 8. The vehicle-to-vehicle gaps reflect how dense drivers are willing to park as well as indicating any available parking spaces. The gap measure could prove useful to researchers and policy makers, e.g., policy decisions can be made between parking density and safety by correlating the gap statistics with property damage claims or accident frequencies. As a result, more effective warrants could be established for the threshold between the use of marked and unmarked parking, or in general refining future parking guidelines to use modifiers that accommodate local conditions. The vehicle length and height information open new opportunities, e.g., it could be possible to classify the parked vehicles (Yang, 2009; Lee and Coifman, 2012) providing a valuable new measure to transportation planners and managers. By also keeping track of the observed vehicle size in a given spot, a change in observed unoccluded vehicle height or length could be used to anonymously track turnover.

4 Conclusions and future work

This paper presented a LIDAR based methodology to monitor parking utilization in unmarked parallel parking areas, though the approach is likely compatible with other ranging sensors, e.g., stereo vision. The work yielded results within 0.8% of ground truth for 1,873 parked vehicles observed over 29 tours. To achieve this low error rate a simple but robust curb detection algorithm was developed, along with basic occlusion reasoning. If deployed on a vehicle already traversing the network, the system could greatly reduce the labor and associated costs incurred to perform parking surveys since it would eliminate the need for dedicated personnel and vehicles. The new data collected by the system could be

[5] Still, on very busy streets it may be necessary to focus on the passenger side, where occlusions can be completely avoided for the same direction parked vehicles (we did not examine this simpler problem in the current study).
[6] Note, when $t_O = t_r$, that q = qm/2.
[7] The utilization is relative to the MUTCD capacity guidelines. Due to the parking zones being unmarked, motorists are at liberty to accept a closer spacing than dictated by the MUTCD, which is why some utilization values are in excess of 100%.

used to help tailor parking supply to better-fit demand (e.g., determining when to install parking meters or adjusting their rates). Alternatively, for a real-time system with fine temporal resolution, the sensors could be mounted on a dedicated probe vehicle driven continuously around a central business district or other area of concern, automatically tallying the parking. In either case, the LIDAR based system offers the promise of yielding previously difficult to collect information about parked vehicles, such as vehicle-to-vehicle gaps, for minimal additional effort.

Data from the passenger side could be collected to estimate same direction parked vehicles, doubling the data collected from a single run and eliminating the possibility of occlusions when the probe is adjacent to the parking lane in its direction of travel (we did not examine this simpler problem in the current study). The present study is meant as a proof of concept. There are many additions and improvements to the system to facilitate widespread use, e.g., refining the curb detection algorithm to automatically find driveways and other areas where parking is prohibited; and combining information across trips or otherwise establish known parking zones to facilitate occlusion reasoning. A separate threshold using length, depth, and height could be applied for the detection of motorcycles in the parking lane. The current study only used rudimentary vehicle length and height measurement algorithms, these could be improved to employ information about the vehicle shape, e.g., Yang (2009) and Lee and Coifman (2012), yielding vehicle class. The vehicle shapes, in turn, would facilitate segmenting closely parked vehicles or deducing that an occluded gap occurred in a contiguous-object containing several vehicles, while also providing a mechanism for anonymously monitoring vehicle turnover. When observing parked vehicles in the opposing direction, as herein, the occlusion reasoning needs to be further developed for occluded vehicle length and height calculations. The present implementation does not consider any LIDAR points in the parking lane if an occlusion is found closer to the probe vehicle, but the methodology could be extended to make use of additional information from the parking lane, e.g., if the top of a parked vehicle is visible throughout an occlusion by a shorter vehicle, one should be able to deduce that no gap occurred in the parking lane during the occlusion. If a second LIDAR is available to form a speed trap, they can be used to efficiently detect moving targets and by combining the two views, see more of the partially occluded vehicles. While the present work used a mounting angle at 90° to the direction of travel, other angles may better facilitate segmenting individual vehicles (e.g., 45° and 135°).

References

Alessandrelli, D., Azzarà, A., Petracca, M., Nastasi, C., Pagano, P., 2012. ScanTraffic: smart camera network for traffic information collection. Wireless Sensor Networks, Springer Berlin Heidelberg, pp. 196-21.

Bickley, W. G., 1968. "Piecewise cubic interpolation and two-point boundary problems." The Computer Journal, 11(2), pp. 206-208.

Chen, L. C., Hsieh, J. W., Lai, W. R., Wu, C. X., Chen, S. Y., 2010. Vision-Based Vehicle Surveillance and Parking Lot Management Using Multiple Cameras. 2010 Sixth International Conference on Intelligent Information Hiding and Multimedia Signal Processing. IEEE, pp. 631–634.

Childs, M.C., 1999. Parking Spaces : A Design, Implementation, and Use Manual for Architects, Planners, and Engineers. McGraw-Hill, New York.

Coric, V., Gruteser, M., 2013. Crowdsensing Maps of On-street Parking Spaces, in: 2013 IEEE International Conference on Distributed Computing in Sensor Systems. IEEE, pp. 115–122.

De Cerreño, A., 2004. Dynamics of On-Street Parking in Large Central Cities. Transportation Research Record, 1898, pp. 130–137.

Deakin, E., Bechtel, A., Crabbe, A., Archer, M., Cairns, S., Kluter, A., Leung, K., Ni, J., 2004. Parking Management and Downtown Land Development in Berkeley , California. Transportation Research Record: Journal of the Transportation Research Board, 1898, pp. 124–129.

Federal Highway Administration, 2007. Advanced Parking Management Systems: A Cross-Cutting Study. Publication FHWA-JPO-07-011.

Federal Highway Administration, 2009. FHWA, Manual on Uniform Traffic Control Devices (MUTCD).

Gray, J., Bell, M., Kuhn, J., 2008. Central City Parking Analysis, Portland Oregon. Project No. 9363. City of Portland Office of Transportation.

Guo, L., Huang, S., Sadek, A.W., 2013. A novel agent-based transportation model of a university campus with application to quantifying the environmental cost of parking search. Transportation Research Part A: Policy and Practice, 50, pp. 86–104.

Institute of Transportation Engineers, 2011. Parking Occupancy - Data Collection. http://www.ite.org/parkinggeneration/datacollection.asp. Accessed 11/10/2011.

Jabbour, M., Bonnifait, P. 2006. Global localization robust to GPS outages using a vertical ladar. 9th International Conference on Control, Automation, Robotics and Vision, Singapore, 5-8 Dec. 2006, pp. 1-6.

Jabbour, M., Bonnifait, P., 2008. Backing up GPS in urban areas using a scanning laser. 2008 IEEE/ION Position, Location and Navigation Symposium, Monterey, CA, 5-8 May 2008, pp. 505-510

Kokolaki, E., Karaliopoulos, M., Stavrakakis, I., 2011. Value of information exposed: wireless networking solutions to the parking search problem. Eighth International Conference on Wireless On-Demand Network Systems and Services (WONS), Bardonecchia, Italy, 26-28 Jan. 2011, pp. 187-194

Lautso, K., 1981. Mathematical Relationships Among Parking Characteristics and Revising and Reduction Methods of Parking Field Survey Information. Transportation Research Part B: Methodological, 15 (2), pp. 73-83.

Lee, H., Coifman B., 2012. Side-Fire LIDAR Based Vehicle Classification. Transportation Research Record, 2308, pp. 173–183.

Liu, Z., Wang, J., Liu, D., 2013. A New Curb Detection Method for Unmanned Ground Vehicles Using 2D Sequential Laser Data. Sensors, 13(1), pp. 1102-1120.

Marsden, G., 2006. The evidence base for parking policies—a review. Transport Policy 13, pp. 447–457.

Marshall, W.E., Garrick, N.W., Hansen, G., 2008. Reassessing On-Street Parking. Transportation Research Record: Journal of the Transportation Research Board, 2046, 45–52.

Mathur, S., Jin, T., Kasturirangan, N., Chandrasekaran, J., Xue, W., Gruteser, M., Trappe, W., 2010. ParkNet: Drive-by Sensing of Road-Side Parking Statistics. 8th international conference on Mobile systems, applications, and services, San Francisco, CA, June 15–18, 2010, pp. 123-136

Ohashi, K, Kimachi, M, Kanayama, K, 1997. Vehicle Recognition from Parking Images using Stereo Method," Proc. of the 4th World Congress on Intelligent Transport Systems, ITS America, 7p.

Olsen, M.J., 2013. Guidelines for the Use of Mobile LIDAR in Transportation Applications. Transportation Research Board, Washington D.C.

Peterson, K., Ziglar, J., Rybski, P., 2008. Fast feature detection and stochastic parameter estimation of road shape using multiple LIDAR. IEEE/RSJ International Conference on Intelligent Robots and Systems, Nice, 22-26 Sept. 2008, pp. 612-619

Pierce, G., Shoup, D., 2013. Getting the Prices Right. Journal of the American Planning Association, 79, 67–81.

Qin, B., Chong, Z. J., Bandyopadhyay, T., Ang, M. H., Frazzoli, E., Rus, D., 2012. Curb-intersection feature based Monte Carlo Localization on urban roads. 2012 IEEE International Conference on Robotics and Automation (ICRA), Saint Paul, MN, 14-18 May 2012, pp. 2640-264

Rodier, C.J., Shaheen, S. a., 2010. Transit-based smart parking: An evaluation of the San Francisco Bay area field test. Transportation Research Part C: Emerging Technologies, 18, pp. 225–233.

Schmid, M.R., Ates, S., Dickmann, J., von Hundelshausen, F., Wuensche, H.J., 2011. Parking space detection with hierarchical dynamic occupancy grids. 2011 IEEE Intelligent Vehicles Symposium (IV) 254–259.

Shoup, D.C., 2006. Cruising for parking. Transport Policy, 13, pp. 479–486.

Suhr, J.K., Jung, H.G., 2013. Sensor Fusion-Based Vacant Parking Slot Detection and Tracking. IEEE Transactions on Intelligent Transportation Systems, article in press, doi:10.1109/TITS.2013.2272100, 16p.

Vickrey, W., 1954. The economizing of curb parking space. Traffic Engineering Magazine, November, pp. 62–67.

Wanayuth, S., Ohya, A., Tsubouchi, T., 2012. Parking Place Inspection System Utilizing a Mobile Robot with a Laser Range Finder -Application for occupancy state recognition. 2012 IEEE/SICE International Symposium on System Integration (SII), pp. 55–60.

Wijesoma, W., Kodagoda, K., Balasuriya, A., 2004. Road-boundary detection and tracking using ladar sensing. IEEE Transactions on Robotics and Automation, *20*(3), pp. 456-464.

Yang, R., 2009. Vehicle Detection and Classification from a LIDAR Equipped Probe Vehicle, Master's Thesis. The Ohio State University.

Figures and Tables

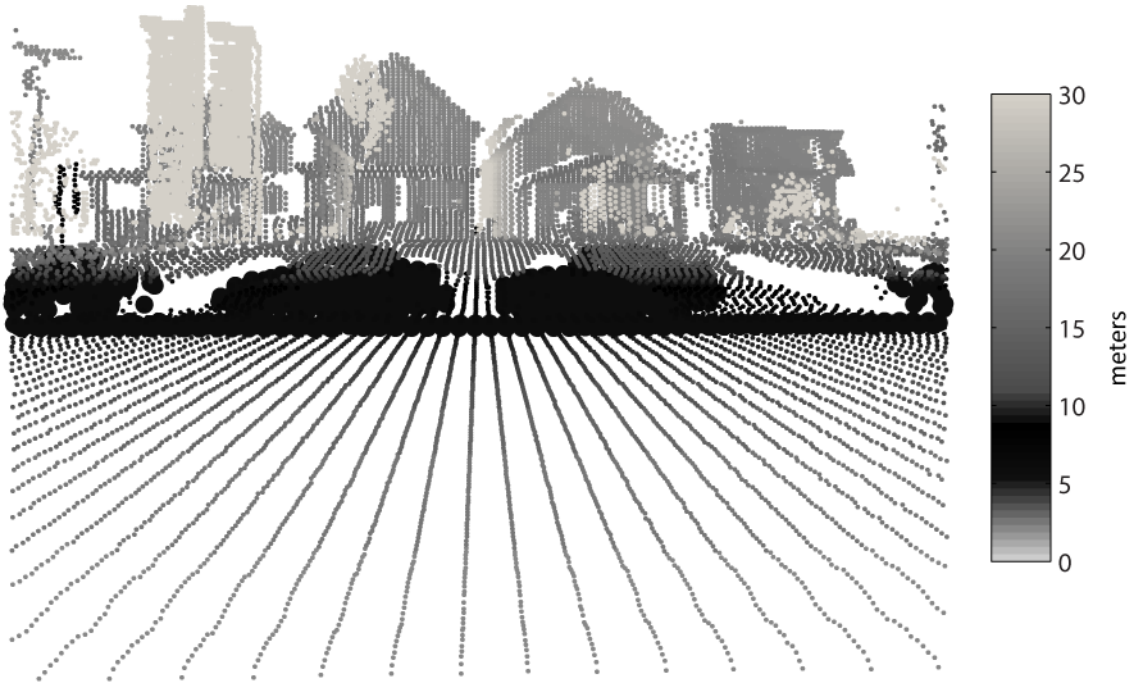

Figure 1. Example of the LIDAR point cloud from the driver-side LIDAR. Scans are made at 37 Hz, in this case the probe vehicle is traveling near the posted speed limit, resulting in the scan lines being approximately 0.1 m apart in this figure. In general the spacing is dependent upon the probe's speed.

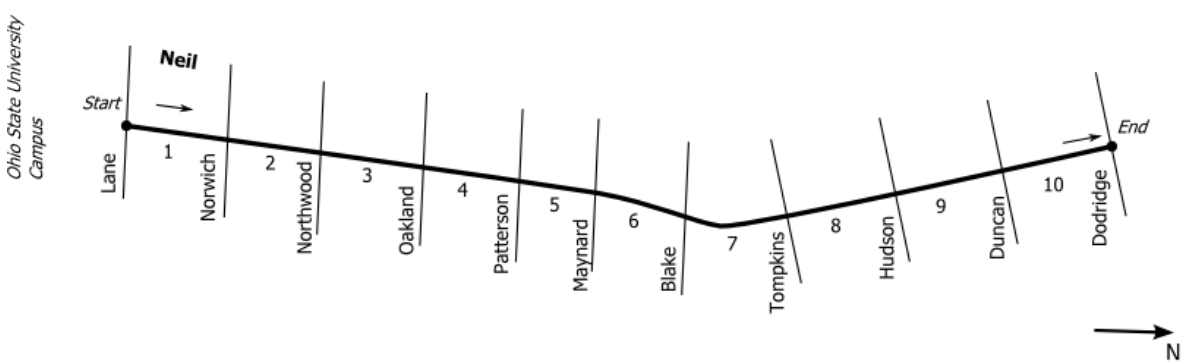

Figure 2. Map of the study location showing the 10 segments, and the total distance from start to end is approximately 1.2 km.

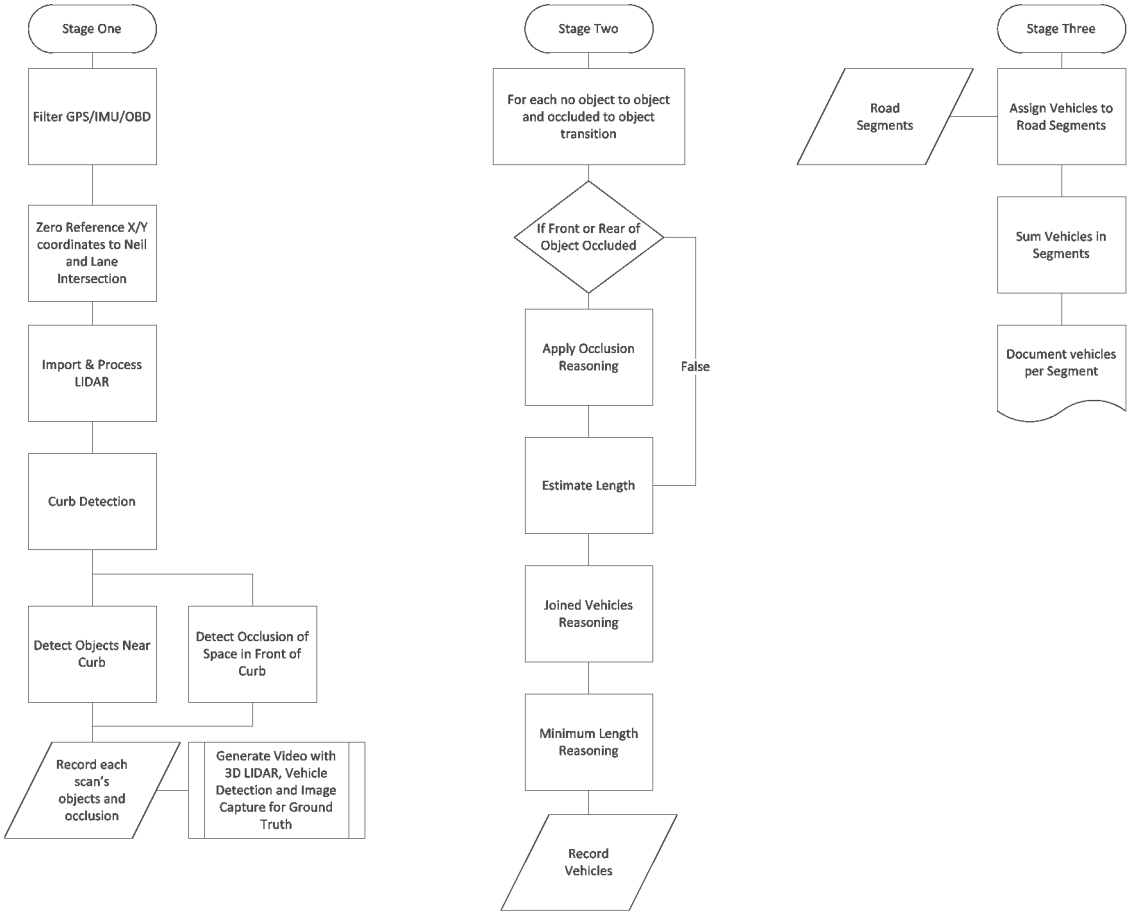

Figure 3. Flow chart of the three stages of the algorithm

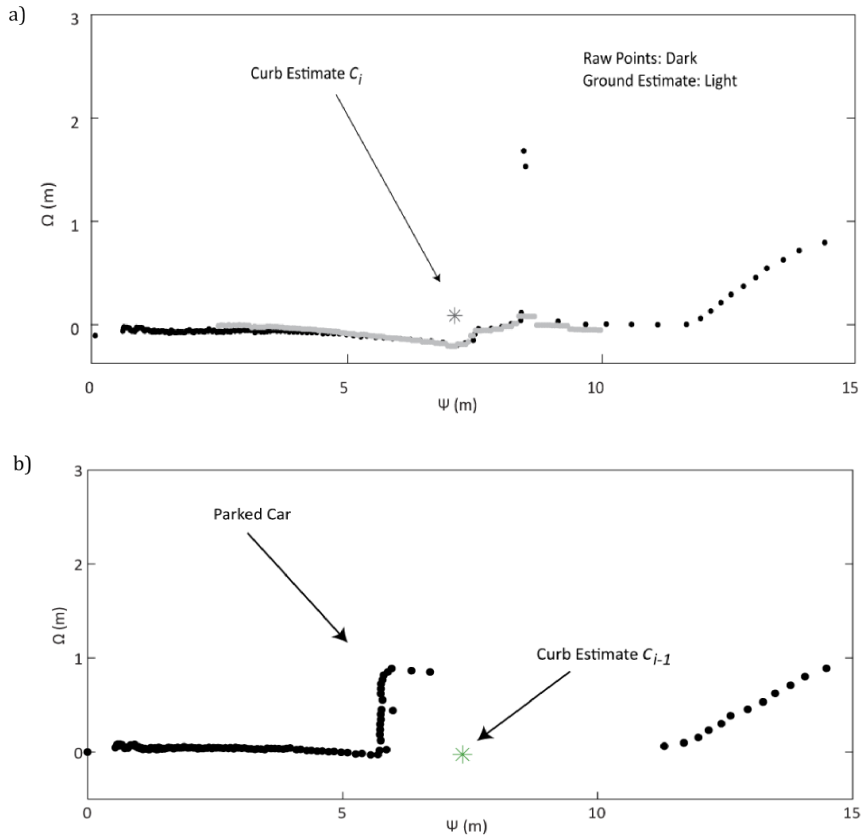

Figure 4. a) The raw LIDAR points, ground points, and curb estimate updated for the current time sample, C_i, resulting from a single scan. b) Raw LIDAR points in a single scan when a vehicle occludes the curb and the corresponding curb estimate using the estimate from the previous time sample, C_{i-1}.

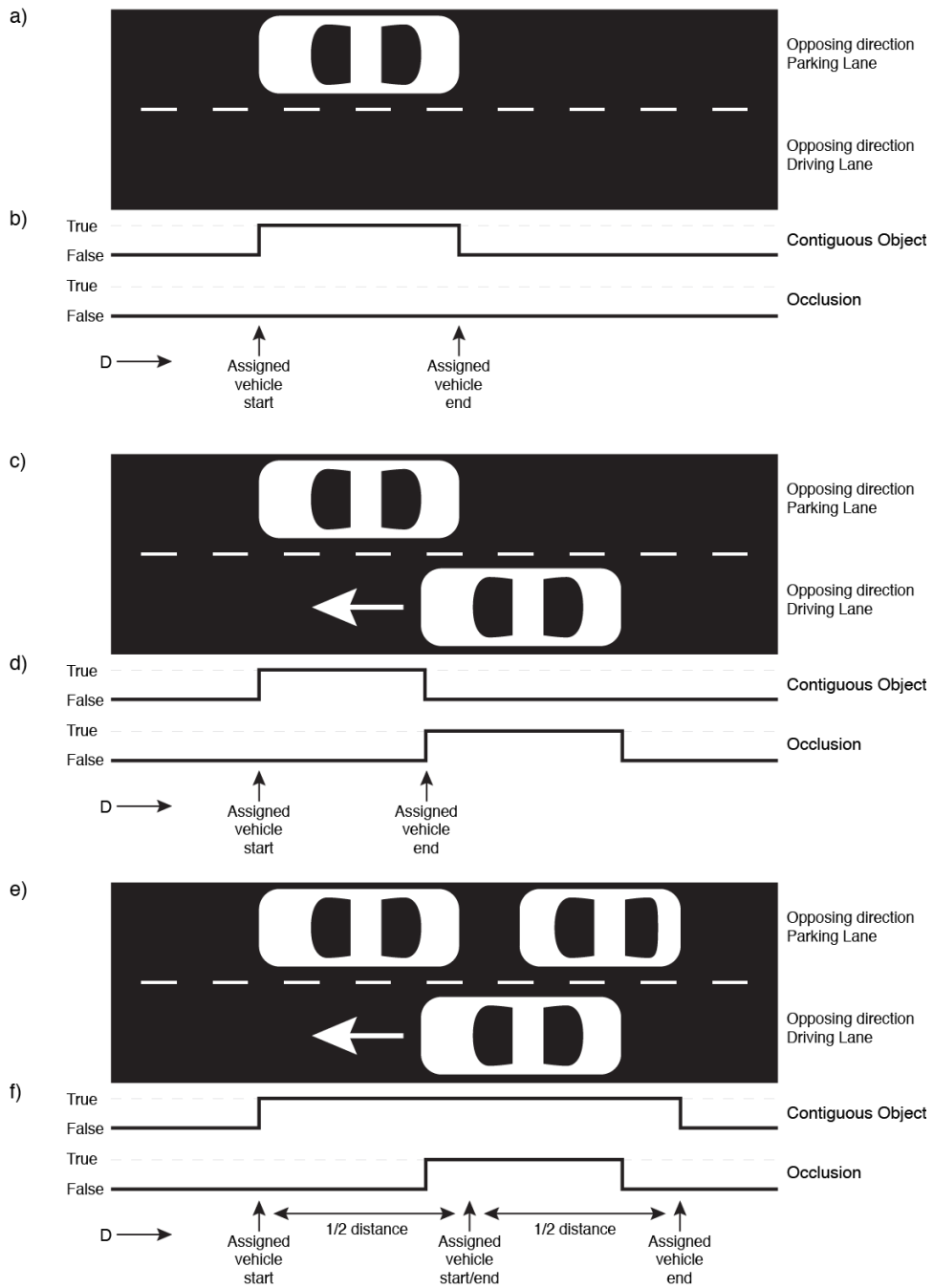

Figure 5. (a) A top-down view of the pair of opposing lanes viewed by the LIDAR, with parking in the top-most of the two. The probe vehicle is not shown in the schematic, it is traveling from left to right in what would be the third lane, across the bottom of the schematic, and (b) the resulting object and occlusion detection by the algorithm in this case. (c) Repeating [a] for a single parked vehicle with an endpoint occlusion, and (d) the resulting object and occlusion detection by the algorithm in this case. Note how the assigned vehicle end falls at the start of the occluder rather than the end of the parked vehicle. (e) Repeating [a] when the gap between two parked vehicles is occluded, and (f) the resulting object and occlusion detection by the algorithm in this case. Note that the assigned vehicle end/start may differ from the actual-but-unobserved end and start.

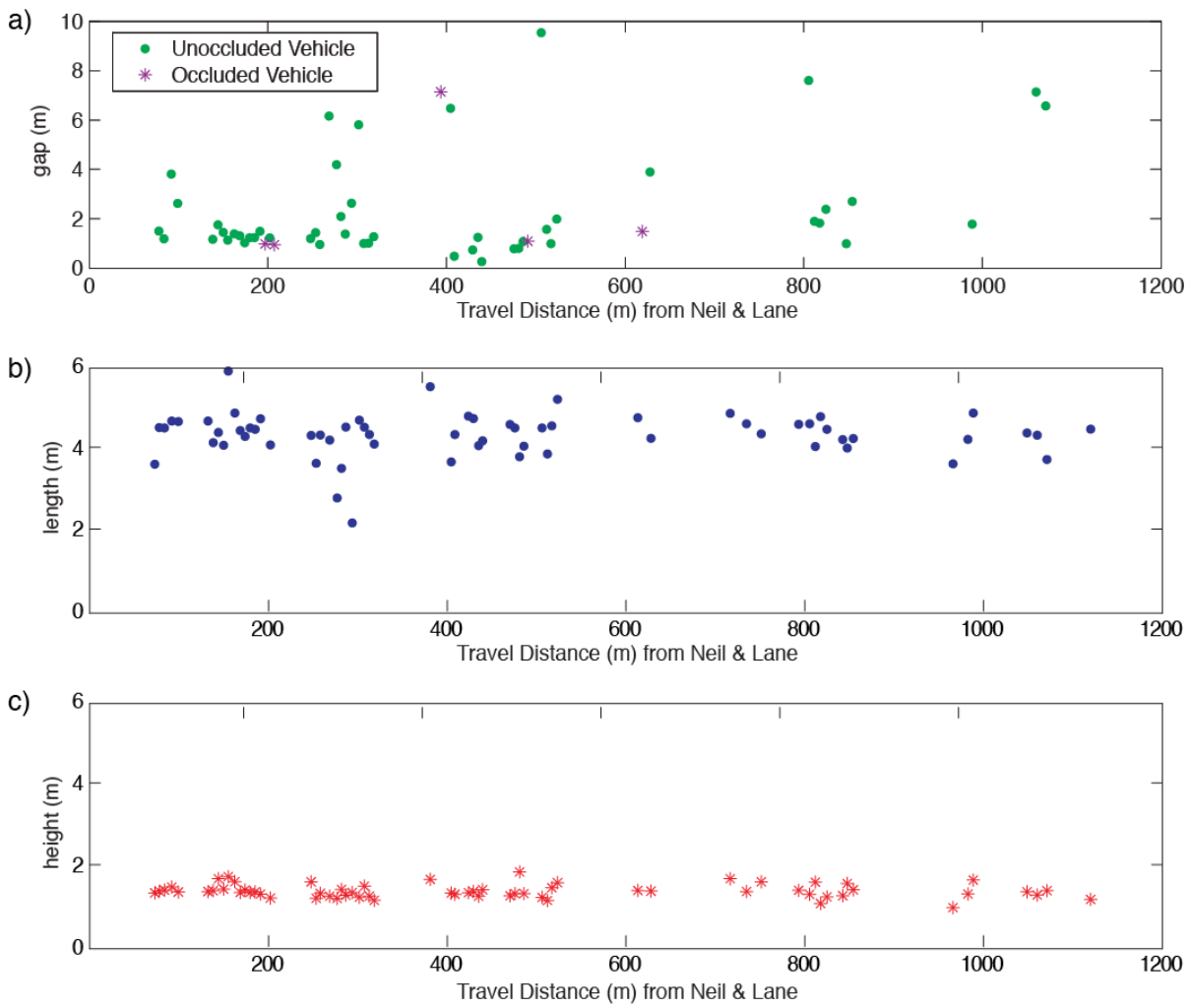

Figure 6. (a) Vehicle-to-vehicle gaps, (b) vehicle lengths, and (c) vehicle heights versus D for a single tour.

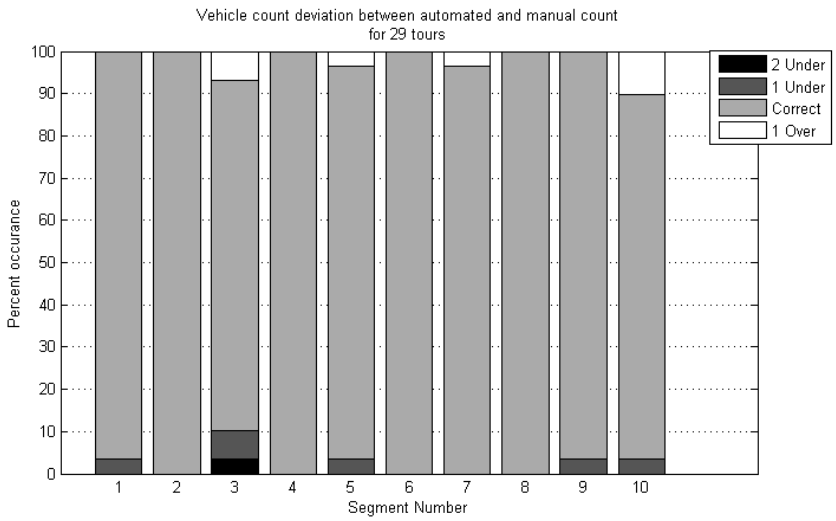

Figure 7. Distribution of the parked vehicle count difference between manual and automatic counts for every segment, across the 29 tours.

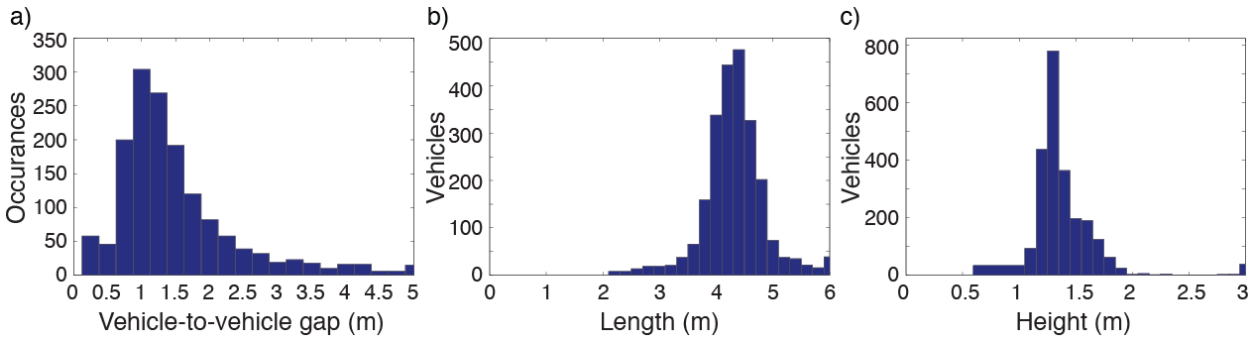

Figure 8. Measured distributions of parked vehicles seen over 29 tours, (a) vehicle-to-vehicle gaps, (b) vehicle length, (c) vehicle height.

Table 1. Comparison of the automated LIDAR based algorithm against ground truth counts by segment across 29 tours.

Segment	Sum of Absolute Errors across runs	Total # of Vehicles	Relative Absolute Error (%)
1	1	171	0.6
2	0	401	0
3	6	357	1.7
4	0	196	0
5	2	237	0.8
6	0	98	0
7	1	85	1.2
8	0	193	0
9	1	31	3.2
10	4	104	3.8
Total	15	1,873	0.8

Table 2. Summary vehicle count and utilization statistics by segment over the 29 tours with ground truth. Note that the utilization is relative to the MUTCD capacity guidelines, which is why some utilization values are in excess of 100%

Segment	1	2	3	4	5	6	7	8	9	10
Capacity	5	12	11	8	9	4	6	11	5	11
Mean Count	5.9	14	12	6.8	8.2	3.4	2.9	6.7	1.1	3.6
Max. Count	7	16	14	8	10	5	6	10	3	6
Min. Count	5	12	10	4	5	1	0	2	0	1
Max. Utilization (%)	140	133	127	100	111	125	100	91	60	55
Mean Utilization (%)	118	115	112	84	91	84	49	61	21	32

Table 3. Average vehicle count and utilization by time of day over 50 tours- the 29 tours with ground truth and an additional 21 tours to increase the subgroup sizes.

	# of Passes	Segment 1	2	3	4	5	6	7	8	9	10
Count Morning	23	6.0	14.2	10.7	6.7	8.2	3.1	3.0	7.3	1.1	3.7
Count Noon	10	6.1	13.5	9.2	6.0	6.4	2.3	2.0	4.8	1.3	3.1
Count Afternoon	17	5.9	13.6	12.4	6.5	8.0	3.8	3.0	6.9	1.0	3.7
Utilization Morning (%)		119	118	98	84	91	77	51	66	23	33
Utilization Noon (%)		122	113	84	75	71	58	33	44	26	28
Utilization Afternoon (%)		119	113	113	82	89	94	50	63	20	34